

---

# EAQuant: Enhancing Post-Training Quantization for MoE Models via Expert-Aware Optimization

---

Zhongqian Fu<sup>1\*</sup>, Ning Ding<sup>3\*</sup>, Kai Han<sup>1</sup>, Xianzhi Yu<sup>1</sup>, Xiaosong Li<sup>2</sup>,  
Xinghao Chen<sup>1</sup>, Yehui Tang<sup>1†</sup>, Yunhe Wang<sup>1†</sup>

<sup>1</sup> Huawei Noah's Ark Lab    <sup>2</sup> Advanced Computing and Storage Laboratory, Huawei

<sup>3</sup> State Key Lab of General AI, School of Intelligence Science and Technology, Peking University  
{fuzhongqian, yehui.tang, yunhe.wang}@huawei.com    dingning@stu.pku.edu.cn

## Abstract

Mixture-of-Experts (MoE) models have emerged as a cornerstone of large-scale deep learning by efficiently distributing computation and enhancing performance. However, their unique architecture—characterized by sparse expert activation and dynamic routing mechanisms—introduces inherent complexities that challenge conventional quantization techniques. Existing post-training quantization (PTQ) methods struggle to address activation outliers, router consistency and sparse expert calibration, leading to significant performance degradation. To bridge this gap, we propose EAQuant, a novel PTQ framework tailored for MoE architectures. Our method systematically tackles these challenges through three key innovations: (1) expert-aware smoothing aggregation to suppress activation outliers and stabilize quantization, (2) router logits distribution alignment to preserve expert selection consistency post-quantization, and (3) expert-level calibration data balance to optimize sparsely activated experts. Extensive experiments across W4A4 and extreme W3A4 quantization configurations demonstrate that EAQuant significantly outperforms existing methods, achieving average score improvements of 1.15 - 2.28% across three diverse MoE architectures, with particularly pronounced gains in reasoning tasks and robust performance retention under aggressive quantization. By integrating these innovations, EAQuant establishes a new state-of-the-art for high-precision, efficient MoE model compression. Our code is available at <https://github.com/darren-fzq/EAQuant>.

## 1 Introduction

Recent advancements in large language models (LLMs) have been significantly influenced by the Mixture-of-Experts (MoE) architecture [20, 13, 5, 27, 28, 6, 7], which leverages dynamic routing mechanisms to scale model parameters efficiently while maintaining sub-linear increases in computational requirements. MoE models achieve superior performance by activating only a subset of expert networks based on input-specific needs, thereby enabling the development of larger models within the constraints of limited computational resources. However, despite their efficiency during training, MoE models face substantial challenges in deployment due to high memory and computational overhead [2, 17]. Specifically, the need to load all experts into memory simultaneously, even when only a few are activated, results in significant memory bandwidth constraints and increased inference costs. These challenges necessitate the exploration of effective compression techniques to reduce memory and computational demands, thereby facilitating the deployment of MoE models on resource-constrained devices.

---

\*Equal Contribution.    †Corresponding Author.

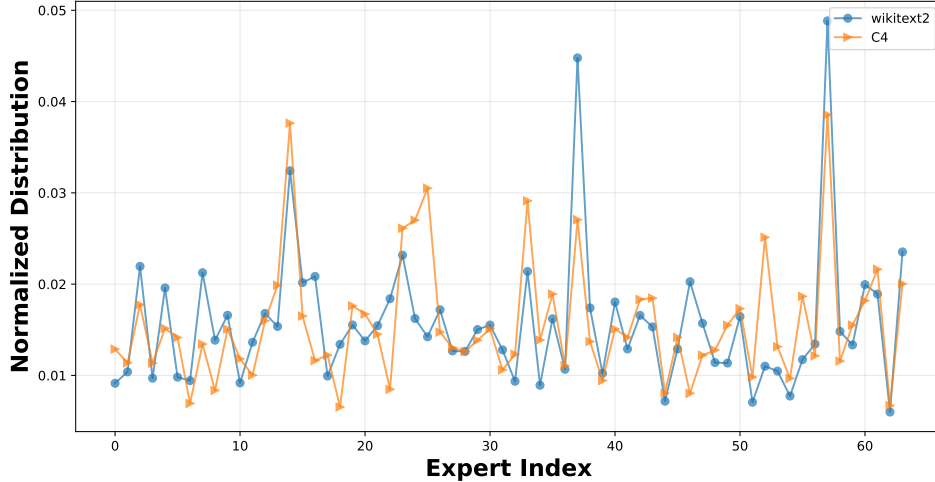


Figure 1: Sample distribution on the first MoE layer of DeepSeek-MoE-16B with different calibration sets. For C4 and WikiText2,  $128 \times 4096$  tokens were sampled.

Post-Training Quantization (PTQ), a method that converts weights and activations to low-precision formats, has demonstrated significant effectiveness in reducing both model size and memory consumption, particularly showing strong performance in traditional large language models (LLMs). However, Quantizing Mixture-of-Experts (MoE) models introduces unique challenges rooted in their sparse, dynamic computation patterns. First, activation outliers in MoE layers exhibit expert-specific distributions, as tokens are routed to distinct subsets of experts. Traditional activation quantization methods [26, 24, 16, 25, 10, 18], designed for dense architectures where all tokens pass through shared weights, fail to handle these expert-dependent outlier patterns, leading to unstable quantization steps and accuracy collapse. Second, the router’s expert selection mechanism is highly sensitive to quantization-induced logit perturbations. Even minor deviations in gate scores can disrupt the top-k expert assignment logic, degrading model performance due to misrouted tokens. Third, expert activation sparsity creates calibration bottlenecks: rarely activated experts receive insufficient data coverage during parameter calibration, resulting in inaccurate estimation of quantization parameters and large quantization errors. Existing PTQ methods [9, 11, 14, 15, 12, 8] either ignore activation quantization entirely or apply uniform smoothing strategies incompatible with MoE’s sparse routing mechanics, leaving these challenges unaddressed.

To tackle these challenges, we propose a novel **Expert-Aware Post-Training Quantization (EAQuant)** method. Our approach begins with an **expert-aware smoothing aggregation strategy** designed to suppress activation outliers across MoE experts. By constructing a unified channel-wise smoothing vector that aggregates maximum scaling requirements from both expert weights and router logits, we redistribute outlier magnitudes while preserving mathematical equivalence through parameter fusion with preceding normalization layers. To ensure consistent expert selection post-quantization, we introduce **router logits distribution alignment** through a dual-objective calibration process that minimizes both logit reconstruction error and Kullback-Leibler divergence between full-precision and quantized routing probabilities. This guarantees stable top-k expert activation despite quantization-induced perturbations. Finally, we resolve expert-level activation sparsity through **expert-level calibration data balance**, where underutilized experts receive prioritized sampling from augmented datasets until their activation counts meet parity with computationally derived expectations.

Extensive evaluations across diverse MoE architectures and quantization configurations demonstrate that EAQuant achieves state-of-the-art performance. For instance, EAQuant improves average task accuracy by 1.37%, 1.15%, and 1.15% over the sota method DuQuant across the three models under W4A4 quantization, with particularly pronounced gains in reasoning benchmarks (e.g., +2.52% on ARC-E for Mixtral-8x7B) and closer perplexity alignment to full-precision baselines. Critically, EAQuant exhibits superior robustness in extreme W3A4 quantization, mitigating performance degradation. These advancements stem from our expert-aware smoothing aggregation strategy, router logits distribution alignment, and expert-level calibration data balancing, collectively establishing EAQuant as the new benchmark for efficient, high-precision MoE quantization.

## 2 Motivation

**Expert-Dependent Outlier Heterogeneity.** MoE architectures assign tokens to specialized experts via router gating, inducing expert-specific activation patterns. For instance, experts trained on mathematical reasoning exhibit sparse, high-magnitude outliers in specific feature dimensions, while experts handling linguistic tasks display smoother activation distributions. Conventional global smoothing strategies [26, 24, 16] fail to capture this per-expert heterogeneity, as they apply fixed scaling factors across all experts. This mismatch leads to over-quantization of outlier-prone experts (causing precision loss) and under-utilization of precision for experts with benign distributions.

**Routing Fragility under Quantization Noise.** MoE routers rely on low-dimensional logit vectors to select top-k experts, a mechanism highly sensitive to quantization-induced perturbations. Even minor distortions in expert weights—common in post-training quantization (PTQ)—can destabilize the gate’s decision boundary, causing misrouting errors and propagate errors through subsequent attention layers. Existing PTQ methods [9, 11] treat the router as a passive component, ignoring its interdependence with expert activations during quantization.

**Calibration Data Imbalance for Rare Experts.** MoE models exhibit power-law activation distributions, where a small subset of “core” experts handle majority of tokens, leaving “niche” experts underutilized. During PTQ calibration, rare experts receive insufficient data coverage, causing their quantization parameters (e.g., scaling factors) to overfit to outliers or noise. As shown in Figure 1, we plot the sample distribution on the first MoE layer of DeepSeek-MoE-16B, this imbalance manifests consistently across both calibration sets. Current methods [11, 14, 15, 12, 8] almost ignore this sparsity, which compromise the MoE’s adaptive computation advantage. MoEQuant [9] proposes expert-balanced self-sampling to create a balanced calibration dataset, however generating new calibration data in this manner may compromise the fairness of comparison with other methods to some extent. Therefore, this calibration sparsity remains unaddressed in sota PTQ methods, creating a critical barrier to efficient MoE deployment.

## 3 Method

In this section, we detail the proposed post-training quantization (PTQ) method for Mixture-of-Experts (MoE) architectures. As shown in Figure 2, our method proceeds with three key components. First and foremost, we introduce an expert-aware smoothing aggregation strategy to effectively mitigate activation outliers in MoE inputs, ensuring robust activation patterns for consistent expert participation. Subsequently, we propose a router logit alignment mechanism that preserves expert selection consistency across quantization stages by aligning the probability distributions of pre—and post-quantization router logits. Furthermore, we propose to balance the calibration data for sparsely activated local experts.

### 3.1 Expert-Aware Smoothing Aggregation

Existing literatures regarding the quantization for Mixture-of-Experts models mainly focus on quantizing weights only, while the activations still remain floating-point values. Our method efficiently quantizing both activations and weights by solving two major challenges encountered when quantizing the incoming activation of the MOE module.

In post-training quantization for large language models, a small number of channels in activation tensors usually exhibit abnormal values with extremely large magnitude. Some well-known works like SmoothQuant [26] and OmniQuant [24] utilize the technique of mergeable smoothing vector to scale the dynamic range of activation tensor before quantizing activations during inference. Specifically, the smoothing vector  $s$  is computed per-channel by  $s_j = \max(|\mathbf{x}_j|)^\alpha / \max(|\mathbf{W}_j|)^{1-\alpha}$  to alleviate the outlier value by channelwise scaling  $\tilde{\mathbf{x}} = \mathbf{x} \cdot \text{diag}^{-1}(s)$ , and therefore mitigate the quantization difficulty. Moreover, the smoothing vector  $s$  can be merged into the preceding normalization layer, incurring no extra computation overhead.

However, this technique faces a critical generalizability issue when quantizing activations of MoE model. For a token vector  $\mathbf{x} \in \mathbb{R}^d$  with  $d$  channels, and an MoE layer with  $n$  local experts. The final

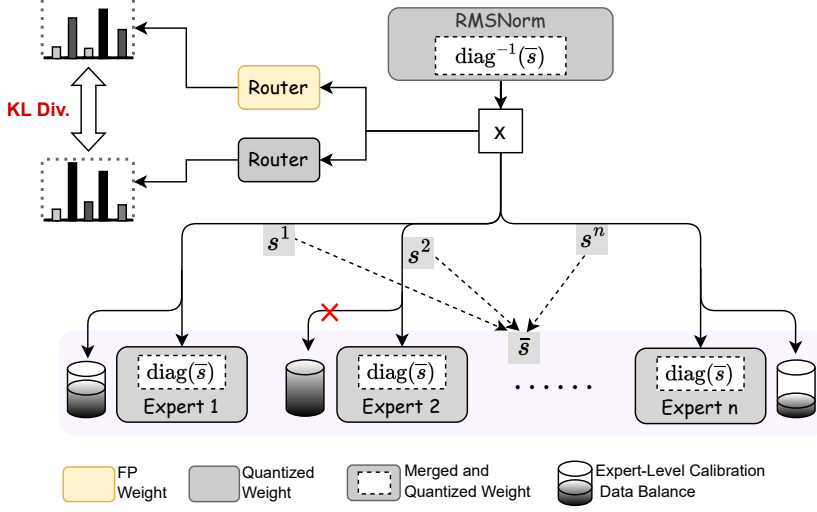


Figure 2: The overview of our proposed EAQuant with three key components. 1) Expert-Aware Smoothing Aggregation. 2) Router Logits Distribution Alignment. 3) Expert-Level Calibration Data Balance.

output of the layer is the weighted sum of selected experts' local outputs by the gate values:

$$\mathbf{y} = \sum_{i \in \mathcal{T}} p^i(\mathbf{x}) E^i(x), \quad (1)$$

where  $\mathcal{T}$  is the set of indices with the highest top-k gate values. In this situation, the original activation smoothing method requires per-expert smoothing vectors  $\{s^i \in \mathbb{R}^d\}_{i=1}^n$  before quantizing activations, respectively computed as:

$$s_j^i = \frac{\max(|\mathbf{x}_j|)^\alpha}{\max(|\mathbf{W}_j^i|)^{1-\alpha}} \quad \forall j \in \{1, 2, \dots, d\} \quad (2)$$

where subscript  $j$  denotes the  $j$ -th input channel and  $\mathbf{W}^i$  denotes the first weight matrix of the  $i$ -th local expert.

While the weight transformation  $\tilde{\mathbf{W}}^i = \mathbf{W}^i \text{diag}(s^i)$  preserves mathematical equivalence through  $\mathbf{x} \mathbf{W}^i = (\mathbf{x} \text{diag}^{-1}(s^i)) \cdot (\text{diag}(s^i) \mathbf{W}^i)$ , the activation scaling operation  $\mathbf{x} \text{diag}^{-1}(s^i)$  must be dynamically executed *after* expert selection, introducing  $\mathcal{O}(kd)$  computational overhead per token where  $k$  is the number of expert each token is routed to. The reason is that the preceding normalizing layer (*i.e.* RMSNorm and LayerNorm) can only absorb one vector before inference.

Our key point is to construct a unified smoothing vector  $\bar{s}$  that satisfies

$$\bar{s}_j \geq \max_{i \in [1, n]} (s_j^i), \quad \forall j \in \{1, 2, \dots, d\}, \quad (3)$$

to suppress the channel-related extreme values in activation no matter which local experts the current token will be routed to. We achieve this through channel-wise maximization over expert-specific requirements:

$$\bar{s}_j = \max_{i \in [1, n]} \left( \frac{\max(|\mathbf{x}_j|)^\alpha}{\max(|\mathbf{W}_j^i|)^{1-\alpha}} \right). \quad (4)$$

This aggregation guarantees that for any selected expert  $i$ , we have

$$\bar{s}_j \geq s_j^i \Rightarrow \text{diag}^{-1}(\bar{s}) \preceq \text{diag}^{-1}(s^i) \quad (5)$$

where  $\preceq$  denotes element-wise inequality, ensuring numerical stability when quantizing the activation with outlier channels.

During the forward propagation of MoE module, the router's weight  $\mathbf{W}^{\text{gate}}$  actually share the same input activation with local experts. Therefore we extend our unified smoothing vector to incorporate

router weights  $\mathbf{W}^{\text{gate}} \in \mathbb{R}^{d \times n}$  by introducing router-specific scaling vector  $s^{\text{gate}} = \frac{\max(|\mathbf{x}_j|)^\alpha}{\max(|\mathbf{W}_j^{\text{gate}}|)^{1-\alpha}}$  into the aggregation process:

$$\bar{s}_j = \max \left( \underbrace{\max_{i \in [1, n]} \left( \frac{\max(|\mathbf{x}_j|)^\alpha}{\max(|\mathbf{W}_j^i|)^{1-\alpha}} \right)}_{\text{Expert requirements}}, \underbrace{\frac{\max(|\mathbf{x}_j|)^\alpha}{\max(|\mathbf{W}_j^{\text{gate}}|)^{1-\alpha}}}_{\text{Router requirement}} \right) \quad (6)$$

This joint maximization guarantees  $\bar{s}_j \geq \max(s_j^{\text{gate}}, \{s_j^i\}_{i=1}^n)$ . The unified scaling enables equivalent transformations for both expert and router computations:

$$\begin{aligned} \text{Router : } \tilde{\mathbf{x}} \tilde{\mathbf{W}}^{\text{gate}} &= (\mathbf{x} \text{diag}^{-1}(\bar{s})) (\text{diag}(\bar{s}) \mathbf{W}^{\text{gate}}) = \mathbf{x} \mathbf{W}^{\text{gate}}, \\ \text{Expert } i : \tilde{\mathbf{x}} \tilde{\mathbf{W}}^i &= (\mathbf{x} \text{diag}^{-1}(\bar{s})) (\text{diag}(\bar{s}) \mathbf{W}^i) = \mathbf{x} \mathbf{W}^i. \end{aligned} \quad (7)$$

And we can absorb  $\bar{s}$  into the preceding RMSNorm layer through parameter fusion

$$\tilde{\mathbf{x}} = \text{RMSNorm}'(\mathbf{x}) = \frac{\gamma \odot \bar{s}}{\sqrt{\frac{1}{d} \sum_{j=1}^d \mathbf{x}_j^2}} \odot \mathbf{x}. \quad (8)$$

### 3.2 Router Logits Distribution Alignment

In order to preserve the accuracy of expert selection for router after quantization, we develop a dual-objective calibration strategy that jointly optimizes numerical precision and routing distribution consistency. Let  $\mathbf{W}^{\text{gate}} \in \mathbb{R}^{d \times n}$  denote the router weights and

$$\mathcal{Q}(\mathbf{W}) = \text{clip}(\text{round}(\frac{\mathbf{W}}{\Delta}) + z, q_{\min}, q_{\max})$$

denotes the uniform quantization operator. Our calibration process solves:

$$\min_{\theta} \underbrace{\mathbb{E}_{\tilde{\mathbf{x}}} [\|\tilde{\mathbf{x}} \tilde{\mathbf{W}}^{\text{gate}} - \tilde{\mathbf{x}} \mathcal{Q}(\tilde{\mathbf{W}}^{\text{gate}})\|_2^2]}_{\text{Logit MSE}} + \cdot \underbrace{\mathbb{E}_{\tilde{\mathbf{x}}} [D_{\text{KL}}(p_{\text{fp}} \| p_{\text{quant}})]}_{\text{Routing KL Divergence}} \quad (9)$$

where  $\theta$  represents quantization parameters such as scale and zero-point for  $\mathbf{W}^{\text{gate}}$ . The probability distributions are computed as:

$$p_{\text{fp}} = \text{softmax}(\tilde{\mathbf{x}} \tilde{\mathbf{W}}^{\text{gate}}) \quad (10)$$

$$p_{\text{quant}} = \text{softmax}(\tilde{\mathbf{x}} \mathcal{Q}(\tilde{\mathbf{W}}^{\text{gate}})) \quad (11)$$

In quantization scenario, even small logit errors can dramatically alter the result of top-k expert selection. The traditional MSE objective solely calibrates the absolute difference of logit magnitudes before and after quantization, while the added Kullback-Leibler (KL) divergence term explicitly minimizes the distribution discrepancy in expert selection probabilities, which is critical for MoE models.

### 3.3 Expert-Level Calibration Data Balance

To address the inherent unbalanced expert activation issue in MoE models during post-training quantization, we propose a dynamic calibration data balancing strategy with expert-balanced sampling. This strategy selects tokens with explicit expert correlation through router configuration analysis and applies threshold-driven oversampling to under-represented experts until their activation counts meet the criterion, enhancing quantization parameter estimation precision.

Following standard PTQ practice, we first sample 128 sequences of length 4096 from WikiText2 to construct the base dataset  $\mathcal{D}_{\text{base}}$ . This data calibrate non-expert components such as the QKV layer and the gating network.

Table 1: Results of DuQuant and ours EAQuant with W4A4 weight-activation quantization configuration among 7 tasks on OLMoE- 7B, DeepSeek-MoE-16B and Mixtral-8x7B. Notably, the router layer is quantized with W8A8.

Model	Method	PPL↓		ACCURACY↑					
		WikiText2	C4	ARC-C	ARC-E	BoolQ	PIQA	WinoGrande	Avg.
OLMoE-7B	FP	7.49	10.52	48.46	78.45	74.56	80.69	69.22	70.28
	DuQuant	8.64	11.51	46.25	74.83	71.28	77.53	63.54	66.69
	EAQuant	8.52	11.41	47.35	76.14	72.29	78.84	65.67	68.06
DeepSeek-MoE-16B	FP	6.51	9.10	47.70	75.88	72.81	80.41	70.40	69.44
	DuQuant	7.10	9.85	43.52	72.43	70.80	76.93	65.67	65.87
	EAQuant	7.06	9.78	44.03	72.90	71.35	78.89	67.96	67.02
Mixtral-8x7B	FP	3.84	6.98	55.80	83.29	84.56	83.41	75.85	76.58
	DuQuant	4.47	7.47	52.22	79.21	81.25	80.74	71.90	73.06
	EAQuant	4.44	7.42	52.13	81.73	82.23	81.07	73.88	74.21

Table 2: Results of DuQuant and ours EAQuant with W3A4 weight-activation quantization configuration among 7 tasks on OLMoE- 7B, DeepSeek-MoE-16B and Mixtral-8x7B. Notably, the router layer is quantized with W8A8.

Model	Method	PPL↓		ACCURACY↑					
		WikiText2	C4	ARC-C	ARC-E	BoolQ	PIQA	WinoGrande	Avg.
OLMoE-7B	FP	7.49	10.52	48.46	78.45	74.56	80.69	69.22	70.28
	DuQuant	10.77	13.59	41.64	70.71	65.75	75.35	63.06	63.30
	EAQuant	10.41	13.20	44.80	73.53	69.27	76.61	63.69	65.58
DeepSeek-MoE-16B	FP	6.51	9.10	47.70	75.88	72.81	80.41	70.40	69.44
	DuQuant	8.28	11.41	40.44	70.20	65.23	76.22	61.64	62.75
	EAQuant	8.19	11.14	42.49	71.17	65.17	75.35	66.22	64.08
Mixtral-8x7B	FP	3.84	6.98	55.80	83.29	84.56	83.41	75.85	76.58
	DuQuant	5.43	8.51	47.35	75.38	77.55	78.62	66.77	69.14
	EAQuant	5.27	8.23	50.68	78.45	78.69	79.05	69.30	71.23

For MoE modules, we first forward  $N = 128 \times 4096$  tokens from  $\mathcal{D}_{\text{base}}$  through the top-k router to obtain the profiling for token-expert assignment. For those experts whose input token quantities are less than the average level of  $r \frac{kN}{n}$  (e.g., the magnification ratio  $r = 2.0$ ) tokens, we iteratively sample new batches from the training dataset to construct  $\mathcal{D}_{\text{expert}}$ , until the routed tokens for these experts all surpass the average level of  $r \frac{kN}{n}$  tokens. Finally we use tokens from  $\mathcal{D}_{\text{base}} \cup \mathcal{D}_{\text{expert}}$  to calibrate the quantization parameters for weights of local experts.

## 4 Experiment

**Models and Evaluations.** We perform comprehensive experiments across three state-of-the-art MoE language models: DeepSeek-MoE-16B [5], OLMoE-7B [20] and Mixtral-8x7B [13]. Beyond conventional perplexity evaluation on the Wikitext-2 [19] and C4 [22] benchmarks, We evaluate the proposed EAQuant on commonsense QA tasks via zero-shot accuracy across four challenging datasets: PIQA [1], ARC [4], BoolQ [3] and WinoGrande [23].

**Baseline.** We choose the sota PTQ method DuQuant [16] as the baseline. The quantization calibration process employs 128 sequentially selected text segments from Wikitext2, with floating-point accuracy results preserved as reference points for performance validation.

**Implementation Details.** In this work, all experiments are done on NVIDIA V100 GPUs with PyTorch [21]. We set sequence length to 2048 for all evaluation tasks. we apply per-token activation quantization and per-channel weight quantization for LLMs. As an effective post-training quantization (PTQ) approach, our proposed EAQuant bypasses the need for parameter-sensitive fine-tuning. We adapt the official repository of DuQuant to support the three MoE models.

Table 3: Influence of different components in EAQuant with W3A4 weight-activation quantization configuration. Notably, the router layer is quantized with W8A8.

Modules			OLMoE-7B			DeepSeek-MoE-16B		
smooth_aggregate	router_align	calib_balance	WikiText2↓	C4↓	Avg.↑	WikiText2↓	C4↓	Avg.↑
✓			10.77	13.59	63.30	8.28	11.41	62.75
			10.47	13.21	65.42	8.21	11.17	63.67
	✓		10.71	13.56	64.20	8.27	11.38	63.15
		✓	10.77	13.58	63.65	8.27	11.39	62.86
✓	✓	✓	<b>10.41</b>	<b>13.20</b>	<b>65.58</b>	<b>8.19</b>	<b>11.14</b>	<b>64.08</b>

## 4.1 Main Results

**Comparison Results.** We conducted comprehensive evaluations of quantization performance across multiple MoE architectures (OLMoE-7B, DeepSeek-MoE-16B, and Mixtral-8x7B) and diverse benchmarks. As demonstrated in Tables 1 and 2, EAQuant consistently outperforms DuQuant under both standard W4A4 and the challenging W3A4 quantization configurations. For W4A4 quantization, EAQuant achieves 1.37%, 1.15%, and 1.15% average score improvements across the three models, with particularly strong gains in reasoning tasks (e.g., +2.52% on ARC-E for Mixtral-8x7B) and better perplexity alignment to full-precision baselines. In the challenging W3A4 regime, EAQuant’s advantages become even more pronounced: it delivers 2.28%, 1.33%, and 2.09% average score improvements over DuQuant, effectively mitigating performance degradation. These results validate EAQuant’s novel expert-aware smoothing aggregation and router alignment strategies, which preserve expert interaction dynamics even under extreme quantization constraints. By achieving state-of-the-art performance across both standard and extreme quantization scenarios, EAQuant sets a new benchmark for efficient MoE model compression.

## 4.2 Ablation Study

**Module-wise Impact.** To evaluate the contributions of individual components in EAQuant, we conduct a module-wise ablation study under the W3A4 quantization configuration (with the router layer fixed at W8A8). In general, we ablate four distinct operations within EAQuant: 1) only the expert-aware smoothing aggregation strategy (smooth\_aggregate); 2) only the router logits distribution alignment (router\_align); 3) only the expert-level calibration data balance (calib\_balance); and 4) full EAQuant approach. The results in Table 3 demonstrate that each component plays a distinct role in enhancing quantized model performance. Specifically, the smooth\_aggregate operation significantly mitigates activation outliers by redistributing outlier magnitudes to the weight domain, leading to a reduction in OLMoE-7B’s WikiText2 perplexity (PPL) from 10.77 to 10.47 and an improvement in its average score from 63.30 to 65.42. For DeepSeek-MoE-16B, it lowers C4 PPL from 11.41 to 11.17 while boosting the average score to 63.67. The router\_align operation moderately improves performance by aligning router logits distributions across experts, increasing OLMoE-7B’s average score to 64.20, while enhancing DeepSeek-MoE-16B’s average score to 63.15. The calib\_balance operation prevents calibration bias across experts, slightly improving OLMoE-7B’s average score to 63.65 and maintaining stability in DeepSeek-MoE-16B. Crucially, the full EAQuant approach, integrating all three components, achieves optimal results. This synergy confirms that smooth\_aggregate addresses activation outliers, router\_align refines expert routing consistency, and calib\_balance ensures balanced expert-level calibration, collectively enabling effective MOE quantization.

**Ablation Analysis of Smooth\_aggregate Strategy.** The ablation results in Table 4 demonstrate the critical role of the smooth aggregate strategy in mitigating performance degradation during post-training quantization (PTQ) for MoE models. Compared to the baseline DuQuant method, which suffers significant drops in both PPL and accuracy, all three variants incorporating specialized aggregation strategies—maximum, expert\_frequency and router\_logits—effectively recover performance. In addition, **maximum** denotes fusion via max-scaling across expert weights, **expert\_frequency** uses weighted sum with activation counts as weights, and **router\_logits** employs weighted sum with routing probabilities as weights. Notably, maximum achieves the strongest overall improvement (+1.20 avg. accuracy), suggesting its effectiveness in preserving critical expert signals during aggregation. Meanwhile, expert\_frequency and router\_logits demonstrate complementary strengths on specific tasks (e.g., ARC-E and WinoGrande), highlighting the importance of balancing expert utilization and

Table 4: Ablation of smooth\_aggregate strategy with W4A4 weight-activation quantization configuration. Notably, the router layer is quantized with W8A8.

Model	Method	PPL↓		ACCURACY↑					
		WikiText2	C4	ARC-C	ARC-E	BoolQ	PIQA	WinoGrande	Avg.
OLMoE-7B	FP	7.49	10.52	48.46	78.45	74.56	80.69	69.22	70.28
	DuQuant	8.64	11.51	46.25	74.83	71.28	77.53	63.54	66.69
	+ maximum	8.54	11.43	<b>47.44</b>	75.04	<b>72.45</b>	<b>79.27</b>	65.27	<b>67.89</b>
	+ expert_frequency	8.56	11.46	45.14	<b>76.09</b>	71.38	78.94	<b>66.06</b>	67.52
	+ router_logits	8.57	11.47	45.99	75.63	71.44	78.45	65.51	67.40

Table 5: Ablation of router\_align in ours EAQuant with different weight-activation quantization configuration among 7 tasks on OLMoE-7B. Notably, Rw\*a\* represents the weight-activation quantization configuration of router layer.

Model	Method	PPL↓		ACCURACY↑					
		WikiText2	C4	ARC-C	ARC-E	BoolQ	PIQA	WinoGrande	Avg.
OLMoE-7B	FP	7.49	10.52	48.46	78.45	74.56	80.69	69.22	70.28
	w3a4_Rw3a4_DuQuant	11.09	13.95	40.70	71.84	62.69	75.24	61.17	62.33
	+ router_align	11.07	13.94	40.87	71.51	67.55	75.73	62.51	63.63
	w3a4_Rw4a4_DuQuant	10.94	13.68	40.70	71.25	64.98	75.63	62.43	63.00
	+ router_align	10.85	13.67	40.96	71.55	68.04	75.30	64.09	63.99
	w3a4_Rw8a8_DuQuant	10.77	13.59	41.64	70.71	65.75	75.35	63.06	63.30
	+ router_align	10.71	13.56	41.64	71.76	69.08	75.52	62.98	64.20
	w4a4_Rw8a8_DuQuant	8.64	11.51	46.25	74.83	71.28	77.53	63.54	66.69
	+ router_align	8.60	11.48	46.76	75.97	72.14	77.80	67.17	67.97

leveraging router dynamics in MoE quantization. These results underscore the necessity of task-aware aggregation strategies to address expert activation irregularities introduced by quantization, while maintaining the OLMoE-7B model’s core capabilities across diverse benchmarks.

**Ablation Analysis of Router Alignment.** We further systematically evaluates the impact of the router\_align mechanism within the EAQuant method under varying weight-activation quantization configurations (W3A4, W4A4) on the OLMoE-7B model. As shown in Table 5, removing router\_align consistently degrades model performance across most tasks, particularly in low-bit quantization regimes. For instance, under W3A4 quantization with router layer fixed at W3A4 (w3a4\_Rw3a4), omitting router\_align results in a 1.30-point drop in average accuracy (62.33 vs. 63.63) and notable declines in BoolQ (62.69 → 67.55) and WinoGrande (61.17 → 62.51). This underscores router\_align’s critical role in mitigating quantization-induced routing inconsistencies. When applying higher quantization to the router layer (e.g., W8A8), router\_align consistently maintain the task performance. For w3a4\_Rw8a8, disabling router\_align reduces average accuracy by 0.9 points (63.30 vs. 64.20), with ARC-E accuracy dropping from 71.76 to 70.71. These results highlight that router\_align effectively calibrates expert routing distributions, counteracting precision loss from aggressive quantization.

The ablation results in Table 6 systematically evaluate the impact of KL loss in the router\_align module under W4A4 quantization (router layer: W8A8), revealing critical insights into expert routing optimization. The kl\_top0 configuration restricts the KL divergence calculation to the top-k (specifically top-8) experts’ logits, whereas kl\_top100 incorporates all experts’ logits in the computation. The relationship between the number of experts  $m$  required to be calculated and the ratio  $r$  can be expressed as the formula:  $m = k + \text{int}((n - k) * r)$ . Compared to the DuQuant baseline (Avg. 66.69), incorporating KL loss constrained to the top-8 experts (kl\_top0) achieves the most significant performance gain (Avg. 67.97), particularly enhancing reasoning tasks such as ARC-E (+1.14) and commonsense reasoning in WinoGrande (+3.63), while slightly reducing perplexity on C4 (11.48 vs. 11.51) and WikiText2 (8.60 vs. 8.64). This demonstrates that focusing KL regularization on the top-k experts (k=8) effectively preserves critical routing signals without introducing computational overhead. Gradually expanding KL regularization to include lower-confidence experts (via ratio parameter  $r$ ) degrades performance (Avg. 67.47→67.19 for kl\_top25→kl\_top100), suggesting that

Table 6: Ablation of KL loss in router\_align with W4A4 weight-activation quantization configuration. Notably, the router layer is quantized with W8A8.

Model	Method	PPL↓		ACCURACY↑					
		WikiText2	C4	ARC-C	ARC-E	BoolQ	PIQA	WinoGrande	Avg.
OLMoE-7B	FP	7.49	10.52	48.46	78.45	74.56	80.69	69.22	70.28
	DuQuant	8.64	11.51	46.25	74.83	71.28	77.53	63.54	66.69
	+ kl_top0	8.60	11.48	<b>46.76</b>	75.97	<b>72.14</b>	77.80	<b>67.17</b>	<b>67.97</b>
	+ kl_top25	8.61	11.50	45.39	75.38	71.65	<b>78.73</b>	66.22	67.47
	+ kl_top50	8.63	11.51	46.33	75.08	70.86	78.56	65.90	67.35
	+ kl_top75	8.61	11.49	46.08	<b>76.01</b>	71.07	78.40	66.38	67.59
	+ kl_top100	8.64	11.51	46.50	75.42	71.35	78.13	64.56	67.19

Table 7: Ablation of the magnification ratio  $r$  in calib\_balance with W4A4 weight-activation quantization configuration. Notably, the router layer is quantized with W8A8.

$r$	0.0	1.0	2.0	4.0	8.0
AVG.	66.69	67.10	<b>67.78</b>	67.47	67.32

excessive regularization on less relevant experts introduces noise into the routing mechanism. Notably, kl\_top0 achieves consistent improvements across all tasks, highlighting its superiority in balancing routing precision and model capacity under quantization constraints. These results underscore the importance of strategically limiting KL regularization to high-confidence experts for maintaining task performance in mixture-of-experts architectures.

**Ablation Analysis of Calibration Balance.** we further investigate the impact of the magnification ratio  $r$  in the calibration balance module. The  $r$  dynamically adjusts the minimum token threshold for expert activation calibration, ensuring underutilized experts receive sufficient data to balance their participation during quantization, thereby mitigating activation imbalance in MoE models. The experiments are performed on OLMoE-7B across five tasks, as shown in Table 7. When  $r$  is set to 2.0, the average score across datasets is maximized. Notably, the baseline without calibration balance ( $r = 0.0$ ) exhibits the lowest accuracy, underscoring the critical role of calibration in mitigating quantization-induced errors.

## 5 Conclusion

This work presents EAQuant, a novel post-training quantization framework tailored for Mixture-of-Experts (MoE) models, which systematically addresses activation outliers, router inconsistency, and expert sparsity through expert-aware smoothing aggregation, router logit alignment, and adaptive calibration data balancing. Extensive experiments on OLMoE-7B, DeepSeek-MoE-16B, and Mixtral-8x7B demonstrate that EAQuant achieves state-of-the-art performance, improving average task accuracy by 1.15 - 1.37% under W4A4 quantization and delivering robust 1.33 - 2.28% gains in extreme W3A4 configurations, with particularly significant improvements in reasoning tasks and reduced performance degradation. By preserving expert interactions and routing stability under aggressive quantization, EAQuant establishes a new benchmark for efficient, high-precision MoE compression, enabling practical deployment of sparse large-scale models in resource-constrained environments.

## 6 Limitation and Future Work

While EAQuant enhances PTQ for MoE models under extreme quantization (e.g., W4A4/W3A4), its effectiveness diminishes in ultra-low-bit regimes (e.g., W1A4) due to the inherent trade-off between granularity and sparsity, necessitating QAT for accuracy recovery. However, QAT incurs significant computational cost and training data dependency, limiting deployment in resource-constrained settings. Future work may explore hybrid PTQ-QAT frameworks or expert-specific calibration to balance efficiency and performance.

## References

- [1] Yonatan Bisk, Rowan Zellers, Ronan Le Bras, Jianfeng Gao, and Yejin Choi. Piqa: Reasoning about physical commonsense in natural language, 2019. URL <https://arxiv.org/abs/1911.11641>.
- [2] Weilin Cai, Juyong Jiang, Fan Wang, Jing Tang, Sunghun Kim, and Jiayi Huang. A survey on mixture of experts in large language models. *IEEE Transactions on Knowledge and Data Engineering*, page 1–20, 2025. ISSN 2326-3865. doi: 10.1109/tkde.2025.3554028. URL <http://dx.doi.org/10.1109/TKDE.2025.3554028>.
- [3] Christopher Clark, Kenton Lee, Ming-Wei Chang, Tom Kwiatkowski, Michael Collins, and Kristina Toutanova. Boolq: Exploring the surprising difficulty of natural yes/no questions, 2019. URL <https://arxiv.org/abs/1905.10044>.
- [4] Peter Clark, Isaac Cowhey, Oren Etzioni, Tushar Khot, Ashish Sabharwal, Carissa Schoenick, and Oyvind Tafjord. Think you have solved question answering? try arc, the ai2 reasoning challenge, 2018. URL <https://arxiv.org/abs/1803.05457>.
- [5] Damai Dai, Chengqi Deng, Chenggang Zhao, R. X. Xu, Huazuo Gao, Deli Chen, Jiashi Li, Wangding Zeng, Xingkai Yu, Y. Wu, Zhenda Xie, Y. K. Li, Panpan Huang, Fuli Luo, Chong Ruan, Zhifang Sui, and Wenfeng Liang. Deepseekmoe: Towards ultimate expert specialization in mixture-of-experts language models, 2024. URL <https://arxiv.org/abs/2401.06066>.
- [6] DeepSeek-AI, Aixin Liu, Bei Feng, Bin Wang, Bingxuan Wang, Bo Liu, Chenggang Zhao, Chengqi Deng, Chong Ruan, Damai Dai, Daya Guo, Dejian Yang, Deli Chen, Dongjie Ji, Erhang Li, Fangyun Lin, Fuli Luo, Guangbo Hao, Guanting Chen, Guowei Li, H. Zhang, Hanwei Xu, Hao Yang, Haowei Zhang, Honghui Ding, Huajian Xin, Huazuo Gao, Hui Li, Hui Qu, J. L. Cai, and Jian Liang. Deepseek-v2: A strong, economical, and efficient mixture-of-experts language model, 2024. URL <https://arxiv.org/abs/2405.04434>.
- [7] DeepSeek-AI, Aixin Liu, Bei Feng, Bing Xue, Bingxuan Wang, Bochao Wu, Chengda Lu, Chenggang Zhao, Chengqi Deng, Chenyu Zhang, Chong Ruan, Damai Dai, Daya Guo, Dejian Yang, Deli Chen, Dongjie Ji, Erhang Li, Fangyun Lin, and Fucong Dai. Deepseek-v3 technical report, 2025. URL <https://arxiv.org/abs/2412.19437>.
- [8] Elias Frantar and Dan Alistarh. Qmoe: Practical sub-1-bit compression of trillion-parameter models, 2023. URL <https://arxiv.org/abs/2310.16795>.
- [9] Xing Hu, Zhixuan Chen, Dawei Yang, Zukang Xu, Chen Xu, Zhihang Yuan, Sifan Zhou, and Jiangyong Yu. Moequant: Enhancing quantization for mixture-of-experts large language models via expert-balanced sampling and affinity guidance, 2025. URL <https://arxiv.org/abs/2505.03804>.
- [10] Xing Hu, Yuan Cheng, Dawei Yang, Zukang Xu, Zhihang Yuan, Jiangyong Yu, Chen Xu, Zhe Jiang, and Sifan Zhou. Ostquant: Refining large language model quantization with orthogonal and scaling transformations for better distribution fitting, 2025. URL <https://arxiv.org/abs/2501.13987>.
- [11] Wei Huang, Yue Liao, Jianhui Liu, Ruifei He, Haoru Tan, Shiming Zhang, Hongsheng Li, Si Liu, and Xiaojuan Qi. Mixture compressor for mixture-of-experts llms gains more, 2025. URL <https://arxiv.org/abs/2410.06270>.
- [12] HamidReza Imani, Abdolah Amirany, and Tarek El-Ghazawi. Mixture of experts with mixture of precisions for tuning quality of service, 2024. URL <https://arxiv.org/abs/2407.14417>.
- [13] Albert Q. Jiang, Alexandre Sablayrolles, Antoine Roux, Arthur Mensch, Blanche Savary, Chris Bamford, Devendra Singh Chaplot, Diego de las Casas, Emma Bou Hanna, Florian Bressand, Gianna Lengyel, Guillaume Bour, Guillaume Lample, L  lio Renard Lavaud, Lucile Saulnier, Marie-Anne Lachaux, Pierre Stock, Sandeep Subramanian, Sophia Yang, Szymon Antoniak, Teven Le Scao, Th  ophile Gervet, Thibaut Lavril, Thomas Wang, Timoth  e Lacroix, and William El Sayed. Mixtral of experts, 2024. URL <https://arxiv.org/abs/2401.04088>.
- [14] Young Jin Kim, Raffy Fahim, and Hany Hassan Awadalla. Mixture of quantized experts (moqe): Complementary effect of low-bit quantization and robustness, 2023. URL <https://arxiv.org/abs/2310.02410>.
- [15] Pingzhi Li, Xiaolong Jin, Zhen Tan, Yu Cheng, and Tianlong Chen. Quantmoe-bench: Examining post-training quantization for mixture-of-experts, 2025. URL <https://arxiv.org/abs/2406.08155>.
- [16] Haokun Lin, Haobo Xu, Yichen Wu, Jingzhi Cui, Yingtao Zhang, Linzhan Mou, Linqi Song, Zhenan Sun, and Ying Wei. Duquant: Distributing outliers via dual transformation makes stronger quantized llms, 2024. URL <https://arxiv.org/abs/2406.01721>.

- [17] Jiacheng Liu, Peng Tang, Wenfeng Wang, Yuhang Ren, Xiaofeng Hou, Pheng-Ann Heng, Minyi Guo, and Chao Li. A survey on inference optimization techniques for mixture of experts models, 2025. URL <https://arxiv.org/abs/2412.14219>.
- [18] Zechun Liu, Changsheng Zhao, Igor Fedorov, Bilge Soran, Dhruv Choudhary, Raghuraman Krishnamoorthi, Vikas Chandra, Yuandong Tian, and Tijmen Blankevoort. Spinqant: Llm quantization with learned rotations, 2025. URL <https://arxiv.org/abs/2405.16406>.
- [19] Stephen Merity, Caiming Xiong, James Bradbury, and Richard Socher. Pointer sentinel mixture models, 2016. URL <https://arxiv.org/abs/1609.07843>.
- [20] Niklas Muennighoff, Luca Soldaini, Dirk Groeneveld, Kyle Lo, Jacob Morrison, Sewon Min, Weijia Shi, Pete Walsh, Oyvind Tafjord, Nathan Lambert, Yuling Gu, Shane Arora, Akshita Bhagia, Dustin Schwenk, David Wadden, Alexander Wettig, Binyuan Hui, Tim Dettmers, Douwe Kiela, Ali Farhadi, Noah A. Smith, Pang Wei Koh, Amanpreet Singh, and Hannaneh Hajishirzi. Olmoe: Open mixture-of-experts language models, 2025. URL <https://arxiv.org/abs/2409.02060>.
- [21] Adam Paszke, Sam Gross, Francisco Massa, Adam Lerer, James Bradbury, Gregory Chanan, Trevor Killeen, Zeming Lin, Natalia Gimelshein, Luca Antiga, Alban Desmaison, Andreas Köpf, Edward Z. Yang, Zach DeVito, Martin Raison, Alykhan Tejani, Sasank Chilamkurthy, Benoit Steiner, Lu Fang, Junjie Bai, and Soumith Chintala. Pytorch: An imperative style, high-performance deep learning library. *CoRR*, abs/1912.01703, 2019. URL <http://arxiv.org/abs/1912.01703>.
- [22] Colin Raffel, Noam Shazeer, Adam Roberts, Katherine Lee, Sharan Narang, Michael Matena, Yanqi Zhou, Wei Li, and Peter J. Liu. Exploring the limits of transfer learning with a unified text-to-text transformer, 2023. URL <https://arxiv.org/abs/1910.10683>.
- [23] Keisuke Sakaguchi, Ronan Le Bras, Chandra Bhagavatula, and Yejin Choi. Winogrande: An adversarial winograd schema challenge at scale, 2019. URL <https://arxiv.org/abs/1907.10641>.
- [24] Wenqi Shao, Mengzhao Chen, Zhaoyang Zhang, Peng Xu, Lirui Zhao, Zhiqian Li, Kaipeng Zhang, Peng Gao, Yu Qiao, and Ping Luo. Omniquant: Omnidirectionally calibrated quantization for large language models. *arXiv preprint arXiv:2308.13137*, 2023.
- [25] Yuxuan Sun, Ruikang Liu, Haoli Bai, Han Bao, Kang Zhao, Yuening Li, Jiaxin Hu, Xianzhi Yu, Lu Hou, Chun Yuan, Xin Jiang, Wulong Liu, and Jun Yao. Flatquant: Flatness matters for llm quantization, 2025. URL <https://arxiv.org/abs/2410.09426>.
- [26] Guangxuan Xiao, Ji Lin, Mickael Seznec, Hao Wu, Julien Demouth, and Song Han. Smoothquant: Accurate and efficient post-training quantization for large language models. In Andreas Krause, Emma Brunskill, Kyunghyun Cho, Barbara Engelhardt, Sivan Sabato, and Jonathan Scarlett, editors, *Proceedings of the 40th International Conference on Machine Learning*, volume 202 of *Proceedings of Machine Learning Research*, pages 38087–38099. PMLR, 23–29 Jul 2023.
- [27] Fuzhao Xue, Zian Zheng, Yao Fu, Jinjie Ni, Zangwei Zheng, Wangchunshu Zhou, and Yang You. Openmoe: An early effort on open mixture-of-experts language models, 2024. URL <https://arxiv.org/abs/2402.01739>.
- [28] Tong Zhu, Xiaoye Qu, Daize Dong, Jiacheng Ruan, Jingqi Tong, Conghui He, and Yu Cheng. Llama-moe: Building mixture-of-experts from llama with continual pre-training, 2024. URL <https://arxiv.org/abs/2406.16554>.